

## Supporting information

### **Constructing a surface spinel layer to stabilize the oxygen frame of Li-rich layered oxides**

Xiaoyan Xie, Jiayang Cui, Zhenkun Liu, Zhuo Yao, Xiaokai Ding, Chenyu Liu\* and  
Dong Luo\*

Guangdong Provincial Key Laboratory of Plant Resources Biorefinery, School of  
Chemical Engineering and Light Industry, Guangdong University of Technology,  
Guangzhou 510006, China.

\*Corresponding authors:

Chenyu Liu (cy.liu@gdut.edu.cn); Dong Luo (luodong@gdut.edu.cn)

## List of contents

### 1. Supplementary Figs:

<b>Figure S1.</b> Scanning electron microscope images of various CA-treatment: <b>a)</b> 50g/L CA-treatment and <b>b)</b> 210g/L CA-treatment. ....	1
<b>Figure S2.</b> Transmission electron microscope images of the as-prepared PRI materials. ....	2
<b>Figure S3.</b> Transmission electron microscope images of the as-prepared CA-LR materials. ....	3
<b>Figure S4.</b> Raman spectra before cycling. <b>a)</b> PRI, <b>b)</b> 50g/L-CA, <b>c)</b> 84g/L-CA and <b>d)</b> 210g/L-CA samples. ....	4
<b>Figure S5.</b> Cycle voltammetry curves of the as-prepared pristine material at the scan rate of $0.1 \text{ mV s}^{-1}$ starting from the oxidation process under the 1 <sup>st</sup> and 2 <sup>nd</sup> cycle. ....	5
<b>Figure S6.</b> <b>a)</b> Initial galvanostatic cycling profile of the as-prepared pristine material at the current density of 0.1C. <b>b)</b> Initial dQ/dV image of the PRI at the current density of 0.1 C.....	5
<b>Figure S7.</b> <b>a)</b> Medium voltage versus cycle number plot PRI samples at 1C. <b>b)</b> Normalized charge-discharge curves of the PRI sample in the 10 <sup>th</sup> , 50 <sup>th</sup> , 100 <sup>th</sup> , 150 <sup>th</sup> and 200 <sup>th</sup> cycles at 1 C .....	6
<b>Figure S8.</b> Charge-discharge curves of <b>a)</b> PRI and <b>b)</b> CA-LR materials at 1 C between 2.0 and 4.8 V. ....	6
<b>Figure S9.</b> Cycling performance of the Li-rich material before and after citric acid treatment between 2.0 and 4.8 V with current density of 1 C.....	7
<b>Figure S10.</b> Equivalent electric circuit used to fit the experimental. ....	7
<b>Figure S11.</b> a) Ni 2p, b) Mn 2p, c) P 2p and d) Mn 3s X-ray photoelectron spectroscopy	

spectra after 200 cycles. ....8

**2. Supplementary Tables:**

**Table S1.** Lattice parameters of the samples. ....9

**Table S2.** Occupancy of atoms in PRI and CA-LR sample as calculated by Rietveld refinement. ....10

**Table S3.** Area ratios of peak I, II and III in Raman spectra of the three samples.....11

**Table S4.** Parameters for electrochemical impedance spectroscopy in term of the fitted results. ....11

**Table S5.** Diffusion coefficient of  $\text{Li}^+$  for PRI and CA-LR samples before and after charged to 4.8V. ....11

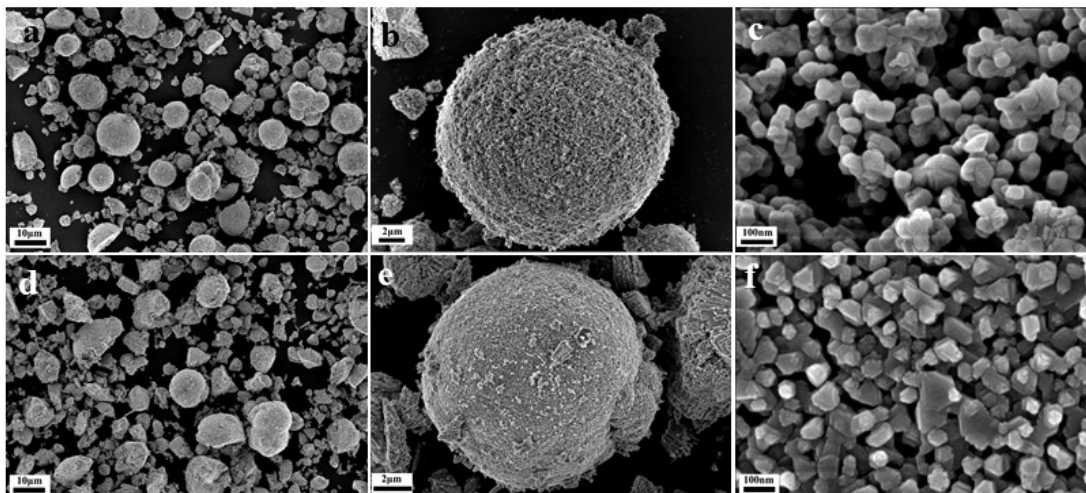


**Figure S1.** Scanning electron microscope images of various CA-treatment: **a)** 50g/L CA-treatment and **b)** 210g/L CA-treatment.

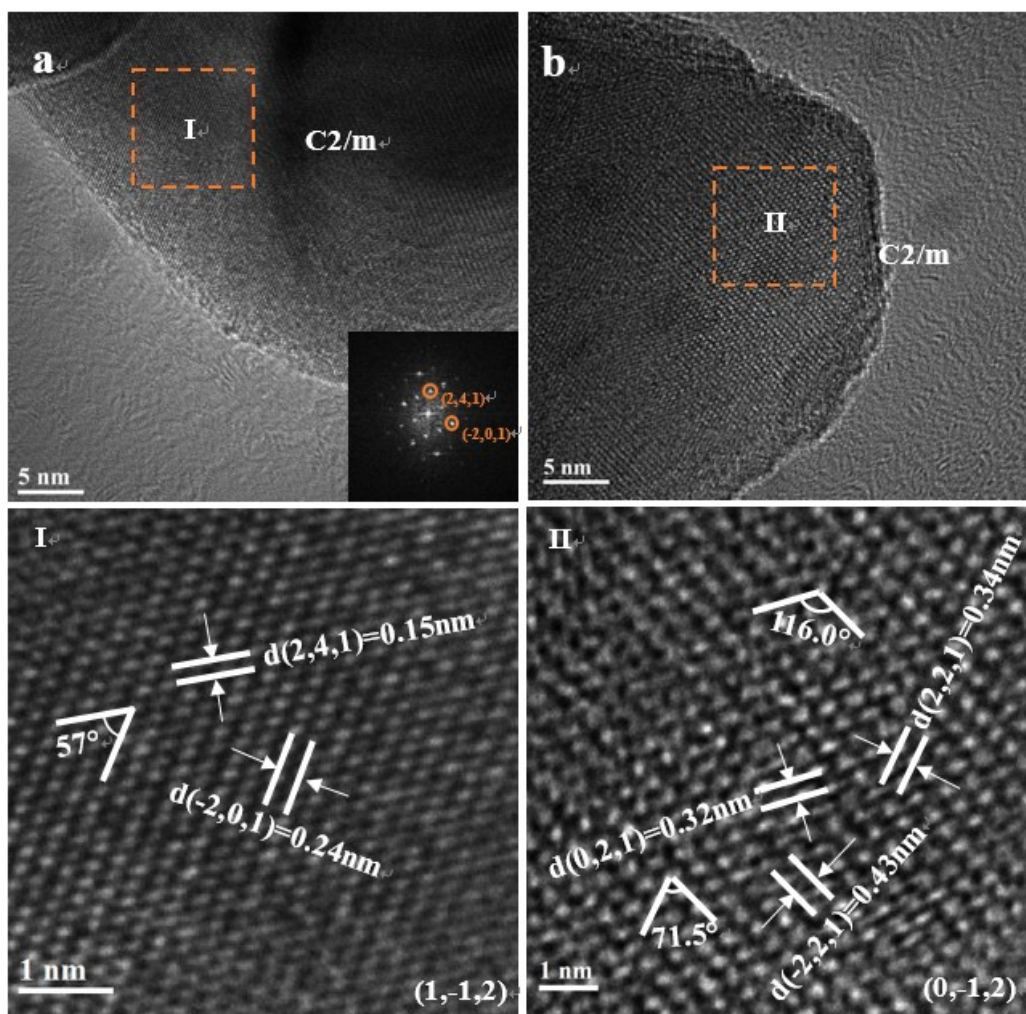


**Figure S2.** Transmission electron microscope images of the as-prepared PRI materials.

**Figure S2** shows a selected domain of the transmission electron microscope images for the as-prepared PRI materials, which belong to the monoclinic structure of  $\text{Li}_2\text{MnO}_3$  with spcing group of  $C2/m$ . Figure S2a shows a zone axis along  $(1,-1,2)$ , which d-spacings was 0.15 and 0.24nm belongs to the  $(2,4,1)$  and  $(-2,0,1)$  planes, respectively, for the angle of  $57^\circ$ , and the slight and sharp FFT pattern was conducted. Another area of the PRI materials showed the  $(0,-1,2)$  zone axis along the  $(0,2,1)$ ,  $(2,2,1)$  and  $(-2,2,1)$  planes, for d-spacing of 0.32nm, 0.34nm and 0.43nm, respectively, and the included angle was  $71.5^\circ$  and  $116.0^\circ$ .

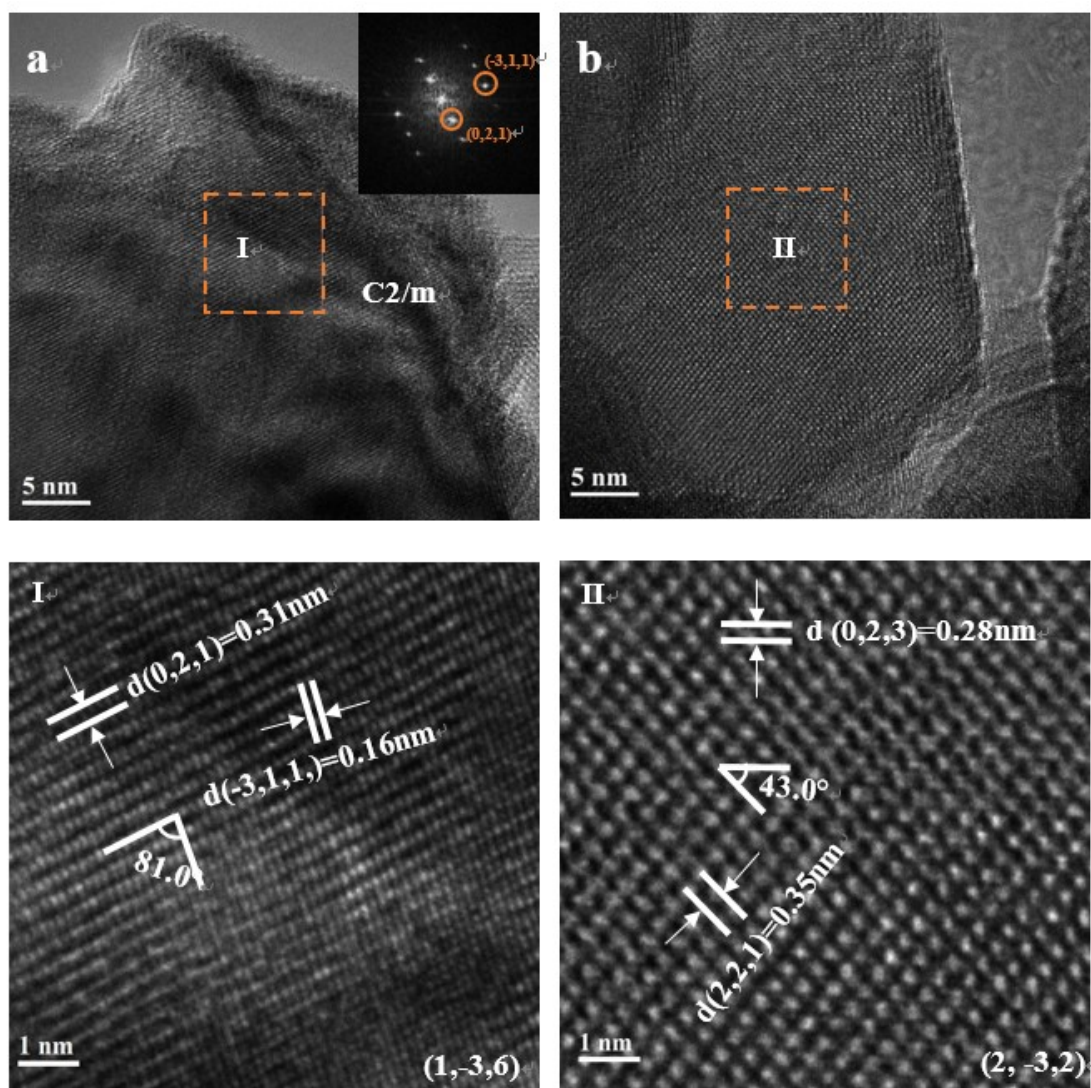


**Figure S3.** Transmission electron microscope images of the as-prepared CA-LR materials.

In addition, **Figure S3a** showed the diffuse streak pattern and the corresponding FFT pattern of the CA-LR materials, indexed to the  $\text{Li}_2\text{MnO}_3$  phase (C2/m spacing group) along the  $(1,-3,6)$  zone axis, and d-spacing of 0.16 and 0.31nm, with the included angle of  $81.0^\circ$ . It was worthy to note that diffuse streak was indistinct, which was due to the treatment of citric acid to pre-activate the  $\text{Li}_2\text{MnO}_3$  phase. Another region in Figure S3b showed the well-defined lattice stripe along  $(2,-3,2)$  zone axis, for d-spacing of 0.35 and 0.28nm, with the angle of  $43.0^\circ$ .

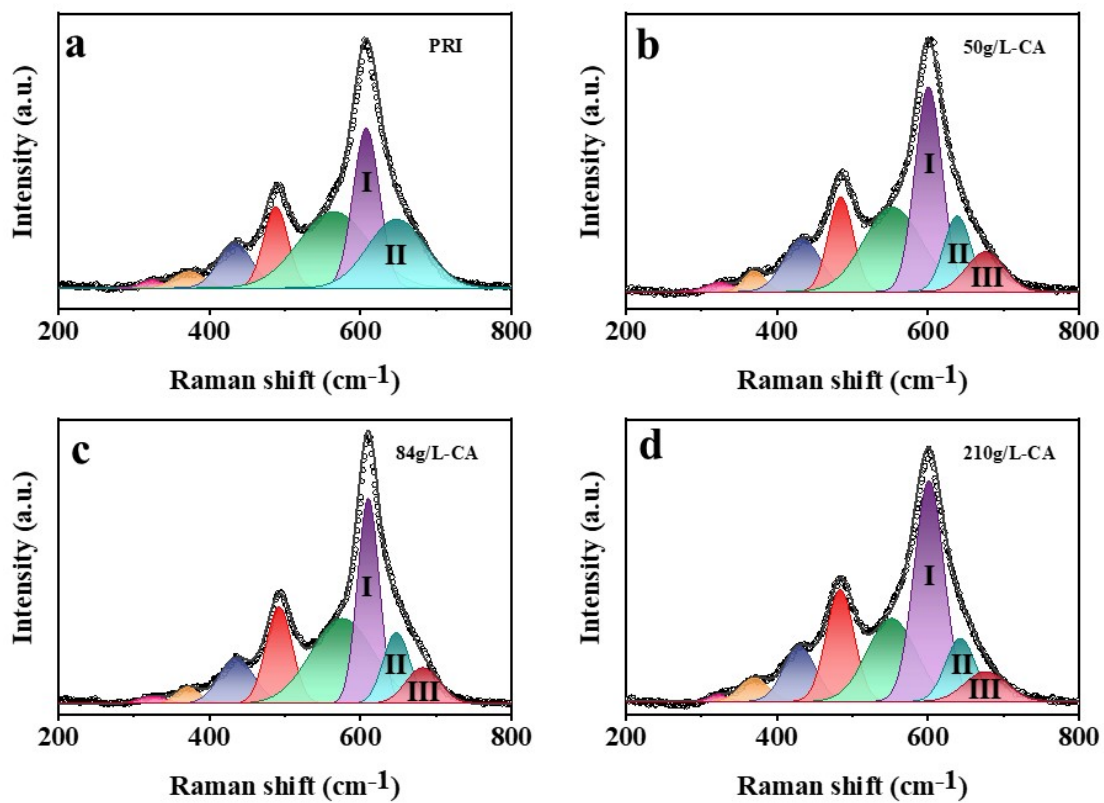


**Figure S4.** Raman spectra before cycling. a) PRI, b) 50g/L-CA, c) 84g/L-CA and d) 210g/L-CA samples.

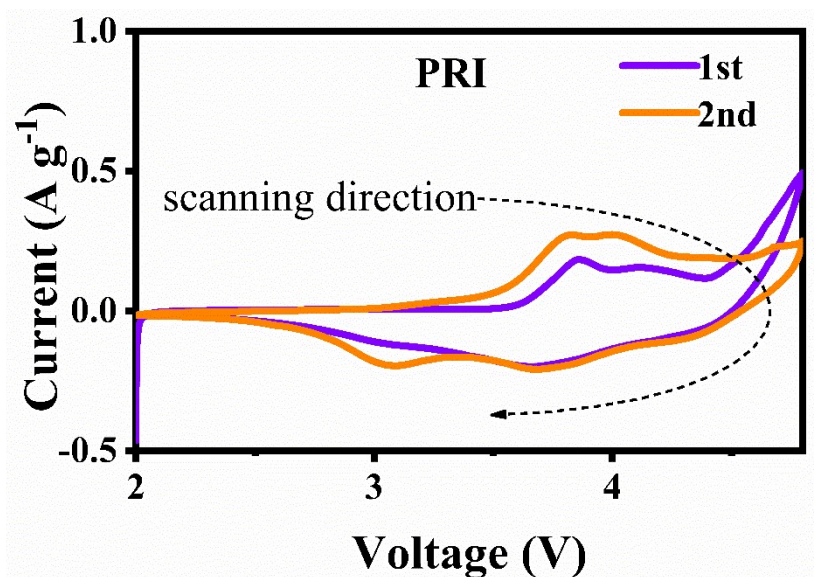


**Figure S5.** Cycle voltammetry curves of the as-prepared pristine material at the scan rate of  $0.1 \text{ mV s}^{-1}$  starting from the oxidation process under the 1<sup>st</sup> and 2<sup>nd</sup> cycle.

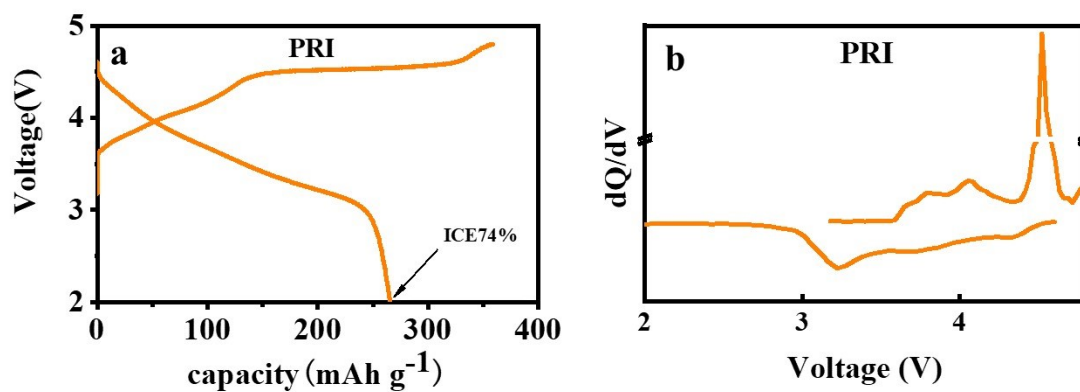


**Figure S6.** a) Initial galvanostatic cycling profile of the as-prepared pristine material at the current density of  $0.1 \text{ C}$ . b) Initial  $dQ/dV$  image of the PRI at the current density of  $0.1 \text{ C}$ .



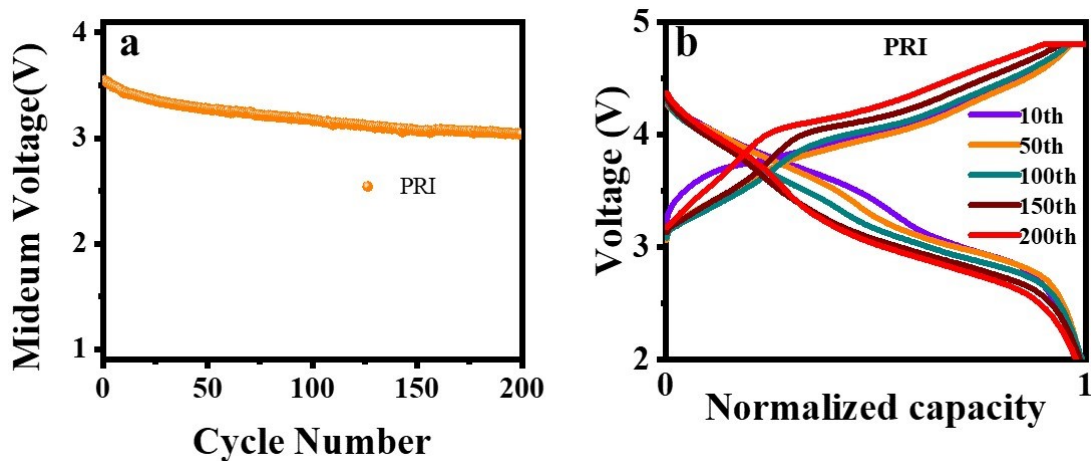


**Figure S7.** a) Medium voltage versus cycle number plot PRI samples at 1C. b) Normalized charge-discharge curves of the PRI sample in the 10<sup>th</sup>, 50<sup>th</sup>, 100<sup>th</sup>, 150<sup>th</sup> and 200<sup>th</sup> cycles at 1 C

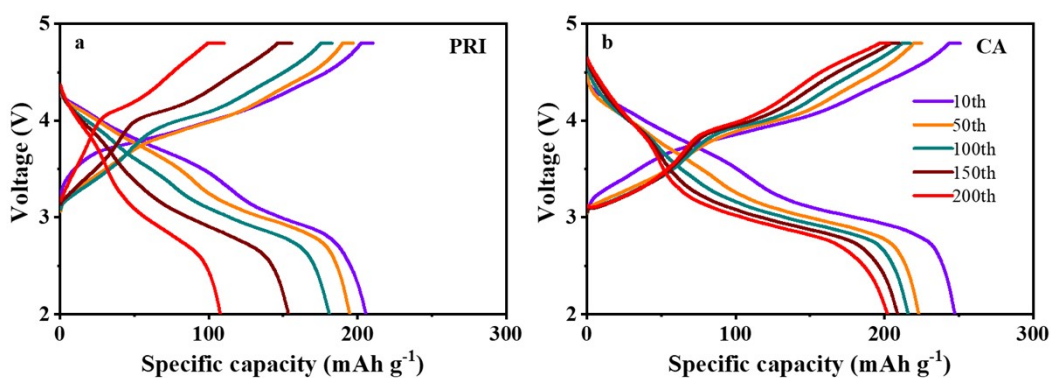


**Figure S8.** Charge-discharge curves of a) PRI and b) CA-LR materials at 1 C between 2.0 and 4.8 V.

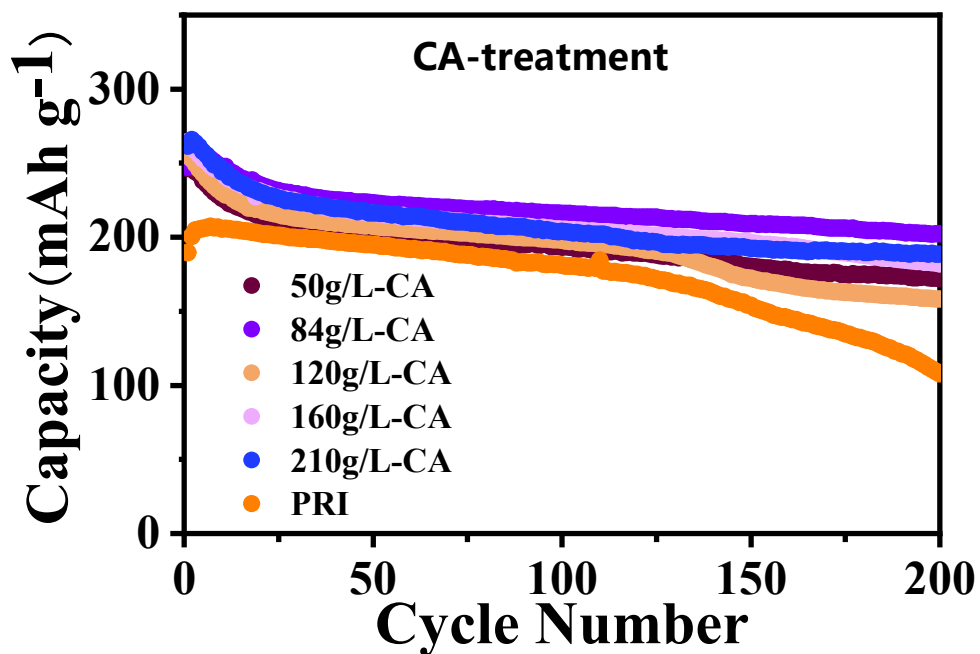


Figure S9. Cycling performance of the Li-rich material before and after citric acid treatment between 2.0 and 4.8 V with current density of 1 C.

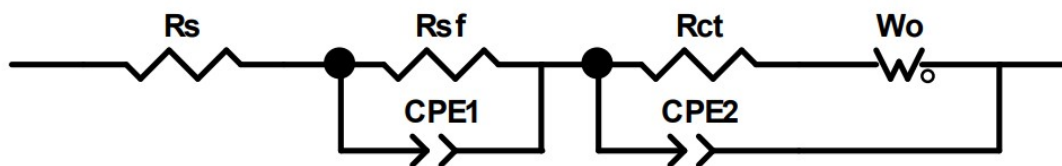
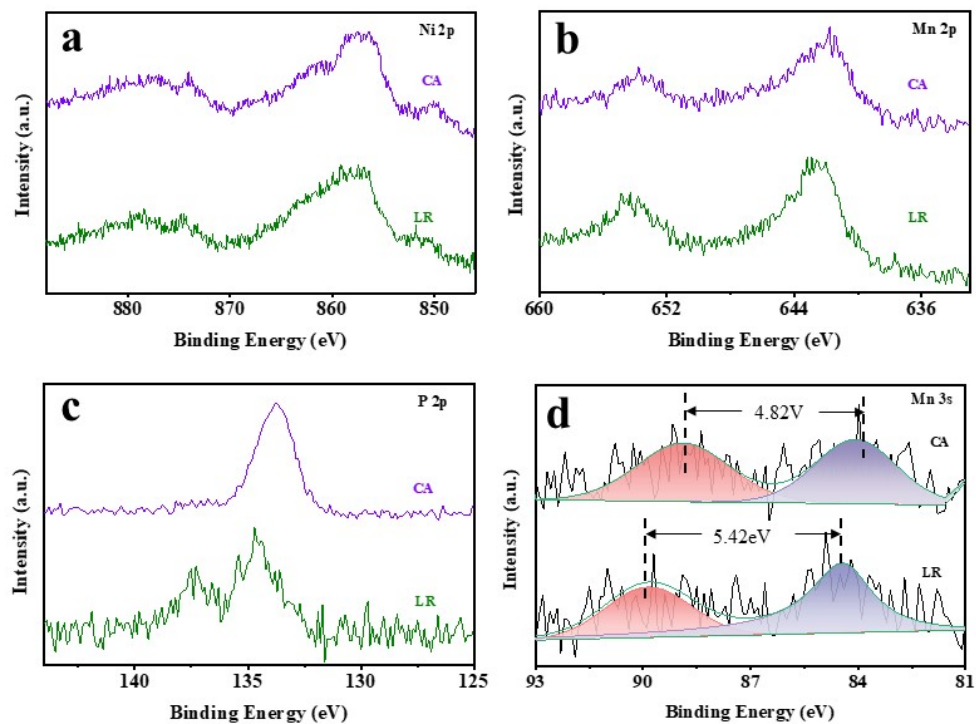


Figure S10. Equivalent electric circuit used to fit the experimental.



**Figure S11.** a) Ni 2p, b) Mn 2p, c) P 2p and d) Mn 3s X-ray photoelectron spectroscopy spectra after 200 cycles.

**Table S1.** Lattice parameters of the samples.

<b>sample</b>			<b>PRI</b>	<b>CA-LR</b>
<b>Lattice parameter</b>	R-3m phase	a(Å)	2.8594	2.8601
		c(Å)	14.2566	14.2649
		V(Å <sup>3</sup> )	100.95	101.06
		c/a	4.9859	4.9876

**Table S2.** Occupancy of atoms in PRI and CA-LR sample as calculated by Rietveld refinement.

<b>Sample</b>	<b>Atom</b>	<b>Site</b>	<b>x</b>	<b>y</b>	<b>z</b>	<b>Occupancy</b>	<b>Mental in Li 3a site</b>
<b>PRI</b>	Li	3a	0	0	0	0.9573	4.27%
	Ni	3a	0	0	0	0.0427	
	Li	3b	0	0	0.5	0.0427	
	Ni	3b	0	0	0.5	0.4573	
	Mn	3b	0	0	0.5	0.5000	
	O	6c	0	0	0.242	1.0000	
<b>Sample</b>	<b>Atom</b>	<b>Site</b>	<b>x</b>	<b>y</b>	<b>z</b>	<b>Occupancy</b>	<b>Mental in Li 3a site</b>
<b>CA-LR</b>	Li	3a	0	0	0	0.9152	8.48%
	Ni	3a	0	0	0	0.0848	
	Li	3b	0	0	0.5	0.0848	
	Ni	3b	0	0	0.5	0.4152	
	Mn	3b	0	0	0.5	0.5000	
	O	6c	0	0	0.242	1.0000	

**Table S3.** Area ratios of peak I, II and III in Raman spectra of the three samples.

<b>sample</b>	<b>Peak I (%)</b>	<b>Peak II (%)</b>	<b>Peak III (%)</b>
<b>PRI</b>	51.4	48.6	0
<b>50g/L-CA</b>	61.0	22.5	16.5
<b>84g/L-CA</b>	58.9	25.0	16.1
<b>210g/L-CA</b>	67.7	19.4	12.9

**Table S4.** Parameters for electrochemical impedance spectroscopy in term of the fitted results.

<b>sample</b>	<b>R<sub>s</sub> (Ω)</b>	<b>R<sub>sf</sub> (Ω)</b>	<b>R<sub>ct</sub> (Ω)</b>	<b>R<sub>total</sub> (Ω)</b>
<b>PRI</b>	2.615	214.8	908.8	1126.2
<b>PRI-4.8V</b>	4.026	86.3	1805	1895.3
<b>CA</b>	1.683	138.2	7.269×10 <sup>-2</sup>	140.0
<b>CA-4.8V</b>	2.196	127.8	407.6	537.6

**Table S5.** Diffusion coefficient of Li<sup>+</sup> for PRI and CA-LR samples before and after charged to 4.8V.

	<b>PRI</b>	<b>PRI-4.8V</b>	<b>CA</b>	<b>CA-4.8V</b>
<b>D (Li<sup>+</sup>)</b>	5.60×10 <sup>-17</sup>	2.19×10 <sup>-16</sup>	9.51×10 <sup>-17</sup>	4.00×10 <sup>-15</sup>